

1 Article

# 2 Production of Cationic Polyacrylamide Flocculant 3 P(AM–DMDAAC) by Microwave Assisted Synthesis, 4 its Characterization and Flocculation Performance

5 Peng Zhang\*, Dongqin Zhao, Xue Zhang

6 School of Civil Engineering, Hunan University of Science and Technology, Xiangtan, Hunan, 411201, China<sup>2</sup>  
7 Affiliation 2; e-mail@e-mail.com

8 \* Correspondence: zhangpeng388@126.com; Tel.: +86-0731-58290251

9 **Abstract:** A composite flocculant P(AM–DMDAAC) was synthesized by the copolymerization  
10 of acrylamide (AM) and dimethyl diallyl ammonium chloride (DMDAAC). Using microwave  
11 (MV) assistance with ammonium persulfate as initiator, the synthesis provided short reaction  
12 time and better solubility product. Nuclear magnetic resonance spectroscopy (<sup>1</sup>H NMR and  
13 <sup>13</sup>C NMR), Fourier-transform infrared spectroscopy (FTIR), scanning electron microscopy  
14 (SEM) and differential thermal analysis-thermo gravimetric analyzer (DTA-TGA) were used to  
15 determine the structure and morphology of P(AM–DMDAAC). Parameters affecting the  
16 intrinsic viscosity ( $[\eta]$ ) of P(AM–DMDAAC), such as microwave time, mass ratio of DMDAAC  
17 to AM, initiator ammonium persulfate dosage, sodium benzoate dosage, bath time, reaction  
18 temperature and pH value were examined. Results showed that the optimum synthesis  
19 conditions were microwave time 1.5 min, m(DMDAAC): m(AM) is 4:16, 0.5 wt% initiator, 0.4  
20 wt% EDTA, 0.3 wt% sodium benzoate, 2 wt% urea, 4 h bath time, 4.0h reaction time and pH 2.  
21 To study the removal of phenol by P(AM–DMDAAC), the influence of flocculant dose, pH  
22 value and the stirring speed were investigated, with optimization providing 99.8 % removal.

23 **Keywords:** acrylamide; microwave assistance; intrinsic viscosity; flocculant; phenol removal

24

## 25 1. Introduction

26 Among the many different pollutants in aquatic ecosystems, phenol is a common toxic  
27 organic compound [1-2]. The toxicity effects of phenol include protein coagulation which could  
28 cause the tissue damage and necrosis in the body, and at low concentrations can denature  
29 proteins [3]. The presence of phenol in industrial wastewater is of concern, due to their wide  
30 utilization in different industries, such as petroleum refining [4-5], resin and plastic production  
31 [6], leather and textile manufacturing, chemical and petrochemical plants, coke ovens, foundry  
32 operations, pulp and paper plants, rubber reclamation plants, pharmaceuticals and  
33 agro-industrial operations [7]. The waste water from these processes can be treated by a number  
34 of physicochemical methods: adsorption, solvent extraction, wet oxidation, heterogeneous  
35 photo catalysis, biological treatments, and advanced oxidation [8-12]. However, the routinely  
36 available methods suffer from serious drawbacks including high cost and the formation of  
37 hazardous byproducts requiring management and disposal. As an alternative, flocculation is  
38 environmental friendly and cost effective strategy, and is an increasingly important process in  
39 pollution control [13-15]. Flocculation is usually the one of the steps in water treatment, and the  
40 final flocculation efficiency determines the kind of flocculant used [16-18]. Consequently,

41 priorities for flocculant and coagulation performance include high efficiency, low cost, and low  
42 environmental impact [19-22].

43 Currently, many organic flocculants are available which include both synthetic and natural  
44 flocculants, such as cationic polyacrylamides (CPAM), anionic polyacrylamides, chitosan and  
45 its derivatives, starch and its derivatives [23-25]. Specifically, CPAM are the subject of increased  
46 attention because of their high efficiency in the purification of drinking water and waste water.  
47 The CPAM family of flocculants are acrylamide based and acrylamide is reactive monomer in  
48 free radical polymerization with extremely good water solubility and is one of the most  
49 cost-effective monomers. They are typical of organic flocculants with electropositive properties  
50 consistent with the presence of acryloyl oxygen ethyl trimethyl ammonium chloride (DAC),  
51 methyl acryloyl oxygen ethyl trimethyl ammonium chloride (DMC) and Dimethyl diallyl  
52 ammonium chloride (DMDAAC) functional groups. The conventional methods of synthesis of  
53 CPAM use a free radical initiator to generate free radical sites on the backbone polymer, with  
54 the reaction of aqueous polymerization initiated by a number of methods including direct heat,  
55 x-rays, microwave (MV), and ultraviolet radiation. Compared with other methods,  
56 MV-initiation has many advantages, such as short reaction time, low dosage of initiator and low  
57 reaction temperature. When using MV- initiation, there are two types method has been used,  
58 the microwave initiated synthesis(no chemical initiator) and microwave assisted synthesis(low  
59 dosage of initiator).

60 This study aimed to investigate the possibility of synthesizing P(AM-DMDAAC)  
61 flocculant by MV assisted initiated polymerization with AM and DMDAAC as monomers. The  
62 synthesis conditions such as microwave time, mass ratio of DMDAAC to AM, dose of  
63 ammonium persulfate, EDTA, sodium benzoate, urea, water bath time, reaction temperature  
64 and pH value were investigated to obtain optimal polymer with high intrinsic viscosity. In  
65 order to study the structural characteristics, nuclear magnetic resonance ( $^1\text{H}$  NMR and  $^{13}\text{C}$   
66 NMR) spectroscopy, fourier-transform infrared (FTIR) spectroscopy, scanning electron  
67 microscope (SEM) and differential thermal analysis-thermo gravimetric analyzer (DTA-TGA)  
68 were used. Finally, the flocculation performance of P(AM-DMDAAC) was evaluated by its  
69 efficiency at removing phenol in a synthetic water sample, under varying. P(AM-DMDAAC)  
70 dose, different pH, and stirring speed .

## 71 2. Materials and Methods

### 72 2.1. Materials

73 Analytical grade EDTA and phenol were purchased from Guangfu Science and  
74 Technology Development Co., Ltd; Analytical grade ammonium persulfate, analytical grade  
75 urea, analytical grade AM and industrial grade dimethyl diallyl ammonium chloride  
76 (DMDAAC) were purchased from Tianjin Kermel Chemical Reagent Co., Ltd; Analytical grade  
77 sodium benzoate was purchased from Tianjin Damao Chemical Reagent. De-ionized water was  
78 used throughout the experiment and pH value of solution was adjusted using NaOH and HCl  
79 solution.

### 80 2.2. Synthesis of P(AM-DMDAAC)

81 The P(AM-DMDAAC) was prepared using AM and DMDAAC as reactive monomer in an  
82 aqueous solution. The reaction was carried out under MV irradiation, and the specific  
83 procedure is as follows. First, a predetermined quantity of AM and DMDAAC were added into  
84 a reaction vessel. Then, deionized water was subsequently added to reach a monomer mass

85 ratio of 30%. The mixture was stirred using a glass rod until the monomers dissolved  
86 completely. Next, the additives EDTA, sodium benzoate and urea were added to the vessel. Not  
87 adjust the pH value, the aqueous solution was purged with pure N<sub>2</sub> at room temperature for 30  
88 min to remove oxygen, and MV-initiator sodium benzoate was added to the vessel. The  
89 reaction vessel was introduced into the WMX-III-A Microwave reactor (Shaoguan KELI  
90 Experiment instrument Co., Ltd., Shaoguan, China) at 20 W for 1.5 min. Then transferred into a  
91 water bath and dried in a vacuum oven at 80 °C.

### 92 2.3. Flocculation Test

93 A ZR 4-6 stirring machine (Shenzhen Zhongran Water Industry Technology Development  
94 Co., Ltd., Shenzhen, China) with six stirrers was used in this experiment. A 200 mL aliquot of  
95 simulated wastewater was transferred into a beaker. Flocculants were dosed under medium  
96 stirring speed of 250 r/min for 4 min, and then changed to the speed of 80 r/min for 10 minutes.  
97 After, settling of 30 minutes, samples were collected from 2 cm below the surface for  
98 measurement using UV-Vis and phenol concentration determined to calculate the removal rate.

### 99 2.4. Characterization of P(AM-DMDAAC)

100 The intrinsic viscosity  $\eta$  of the polymer, expressed in deciliters per gram (dL/g), was  
101 measured in a 1.0 mol/L NaCl solution with an Ubbelohde capillary viscometer (Shanghai  
102 Shenyi Glass Instrument Co. Ltd., China) at  $30 \pm 0.05$  °C. The value of  $\eta$  was determined by one  
103 point method according to the Solomon-Ciuta formula. The <sup>1</sup>H NMR spectrum and <sup>13</sup>C NMR  
104 spectra were obtained with an AVANCE 500 nuclear magnetic resonance spectrometer  
105 (BRUKER Company, Germany), with D<sub>2</sub>O solvent. FTIR spectra were recorded by using  
106 Fourier Transformed Infra Red (FT-IR) Spectrophotometer (Nicolet 6700, Nicolet instrument  
107 Company, USA) with KBr pellets, and polymer morphology was examined by using the  
108 scanning electron microscope (SEM) (JSM-6380LV, JEOL Company, Japan). The thermal  
109 gravimetric analysis (TGA) was conducted at a heating rate of 10 °C·min<sup>-1</sup> under nitrogen flow  
110 of 20 mL·min<sup>-1</sup> over a temperature range from room temperature up to 600 °C on a DTG-60H  
111 synchronal thermal analyzer (SHIMADZU, Japan), in order to investigate the thermal stability  
112 of the copolymer. The concentration of phenol was examined by using UV-Vis  
113 spectrophotometer (TU-1910, Beijing Purkinje General Instrument Co., Ltd, China)

## 114 3. Results

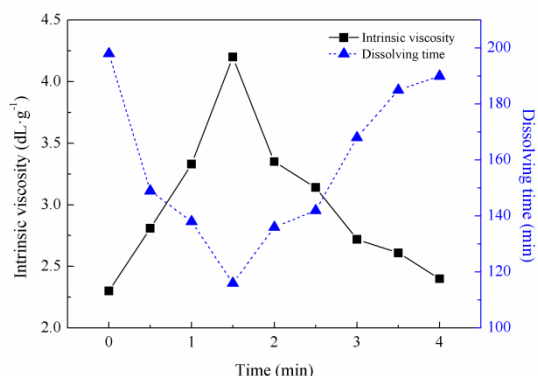
### 115 3.1. Synthesis of P(AM-DMDAAC)

116 Because the intrinsic viscosity is a major determinant in controlling P(AM-DMDAAC)  
117 performance [26], the effectiveness of P(AM-DMDAAC) prepared in this study was assessed  
118 using intrinsic viscosity. Parameters affecting the intrinsic viscosity such as microwave time,  
119 mass ratio, dose of ammonium persulfate; EDTA, sodium benzoate, urea, bath time,  
120 temperature and pH, were examined.

#### 121 3.1.1. Effect of the microwave time on intrinsic viscosity

122 Microwave power is one of the most important factors that affect the properties of polymer  
123 synthesis. Particularly excessive microwave power may cause a fast polymerization, the  
124 temperature of the system to increase quickly, and the heat of polymerization is not easy to  
125 dissipate. Microwave power was fixed at 20 W to minimize these effects. The impact of microwave  
126 time on the intrinsic viscosity of the polymer was investigated. As shown in Figure 1, the intrinsic  
127 viscosity of the polymer exhibits a peak at 1.5 minutes and the intrinsic viscosity of the polymer

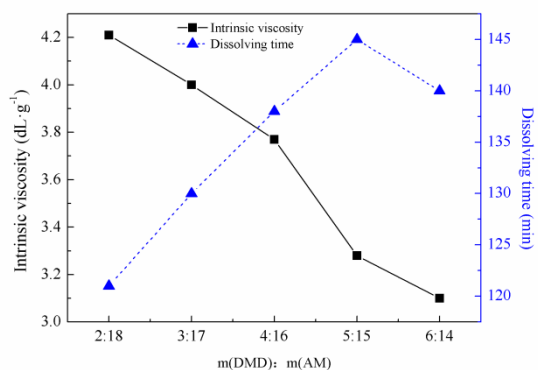
128 reaches a maximum of 4.20 dL/g. For low microwave time it was difficult to provide sufficient  
 129 temperature and the microwave effect in the reaction system, which meant the polymerization chain  
 130 reaction was not established, at longer MV time, the reaction rate increases until an optimum and  
 131 degrades due to the collision probability between free radicals, and at the same time the chain  
 132 reaction becomes easily terminated, which leads the decrease intrinsic viscosity of the P(AM-  
 133 DMDAAC). Therefore, the optimum microwave time was identified as 1.5 min.



134 **Figure 1.** Effect of microwave time on intrinsic viscosity

### 135 3.1.2. Effects of the monomer quality ratio on intrinsic viscosity

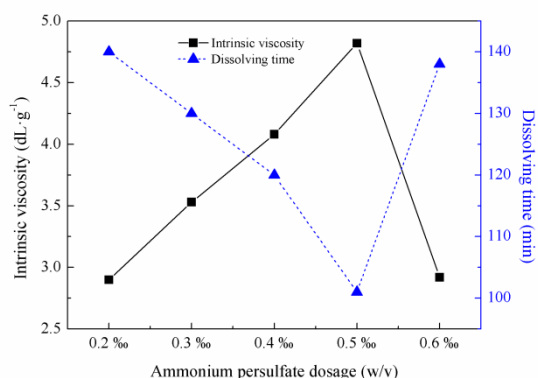
136 The effects of the mass ratio of DMDAAC to AM on the intrinsic viscosity of P(AM-DMDAAC)  
 137 was explored. As shown in Figure 2, the intrinsic viscosity of the polymer decreased with the  
 138 increasing proportion DMDAAC monomer. When m(DMDAAC): m(AM) was 2:18, the intrinsic  
 139 viscosity of the polymer reached the maximum of 4.21 dL/g. This is due to the chemical reactivity of  
 140 cationic monomer DMDAAC being lower than the chemical reactivity of AM. When the initiator  
 141 used was ammonium persulfate, the chemical reactivity ratios of the DMDAAC monomer to the AM  
 142 monomer were  $\gamma_{\text{DMDAAC}} = 0.58$  and  $\gamma_{\text{AM}} = 6.7$ , respectively, which means that the activity of the  
 143 monomer AM was higher than that of DMDAAC monomer. The higher the proportion of DMDAAC  
 144 monomer, the longer the time required to reach the polymerization temperature leading to  
 145 incomplete monomer polymerization. So the intrinsic viscosity of the polymer decreased with the  
 146 increased proportion of the DMDAAC monomer. The cationic degree was also an important factor  
 147 influencing choice of polymer, in general the higher the degree of cationic, the better the water  
 148 treatment effect. Therefore, the optimum m(DMDAAC): m(AM) was 4:16.



149 **Figure 2.** Effect of monomer quality ratio on intrinsic viscosity

### 150 3.1.3. Effect of ammonium persulfate dose on intrinsic viscosity

151 The effects of the dosage of ammonium persulfate on the intrinsic viscosity of P(AM-  
152 DMDAAC) was explored. As shown in Figure 3, the intrinsic viscosity of the polymer exhibits an  
153 optimal point with the increasing proportion of ammonium persulfate. When the proportion of the  
154 initiator ammonium persulfate was 0.5‰ (w/v), the intrinsic viscosity of the polymer reached the  
155 maximum of 4.80 dL/g. When the proportion of the initiator was lower, the concentration of free  
156 radicals and the reaction point were low, so the chain reaction was difficult to initiate and sustain  
157 and the intrinsic viscosity of polymer was lower. With the increasing proportion of the initiator, the  
158 concentration free radicals and the number of the reaction centers increased, which lead to the  
159 reaction rate and the intrinsic viscosity of polymer being higher. However, when the initiator  
160 proportion was too high, the excessive number of free radicals the higher the probability of collision  
161 and chain termination. Moreover, a fast reaction rate may also lead a sudden rise in temperature  
162 with a high susceptibility of implosion and a lower intrinsic viscosity of the polymer. Therefore, the  
163 optimum initiator ammonium persulfate dose was 0.5‰ (w/v).



164 **Figure 3.** Effect of ammonium persulfate dose on intrinsic viscosity

#### 165 3.1.4. Effect of EDTA dose on intrinsic viscosity

166 The industry grade AM monomer can contain metal ions, such as Cu<sup>2+</sup> and Fe<sup>2+</sup> which could  
167 consume primary radicals during reaction. These metal ions may hinder chain propagation and  
168 increase the induction period. The presence of EDTA to a complex with Cu<sup>2+</sup> and Fe<sup>2+</sup>, would  
169 eliminate their influence on the reaction and increasing the intrinsic viscosity of the polymer. The  
170 effects of the proportion of EDTA on the intrinsic viscosity of P(AM-DMDAAC) was explored with  
171 all other conditions given. As shown in Figure 4, the intrinsic viscosity of the polymer showed a  
172 similar optimum with the increasing proportion of the EDTA. When the proportion of EDTA was 0.4  
173 ‰ (w/v), the intrinsic viscosity of the polymer reached the maximum of 4.7 dL/g. When the  
174 proportion of the EDTA was low, metal ions in the reaction system, such as Cu<sup>2+</sup>, Fe<sup>2+</sup>, etc., were in  
175 excess so the polymerization reaction was also be hindered by the metal ions. Conversely, when the  
176 proportion of the EDTA was high, the probability of chain transfer reaction increased, which does  
177 not enhance the intrinsic viscosity and the optimum dose of EDTA was 0.4 ‰ (w/v).

178

179

180

181

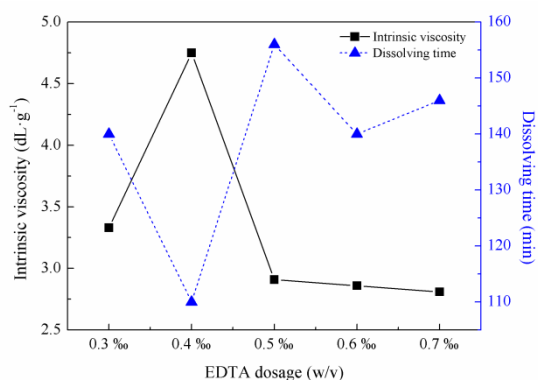
182

183

184

185

186



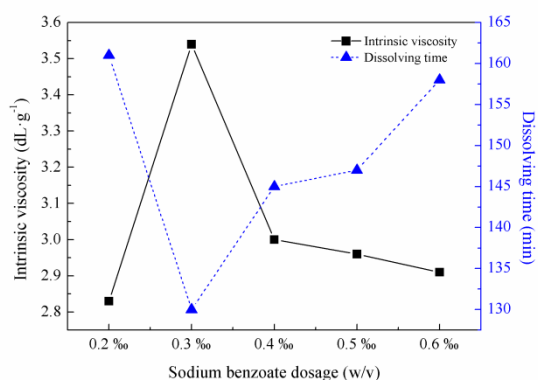
187

**Figure 4.** Effect of EDTA dose on intrinsic viscosity

### 188 3.1.5. Effect of sodium benzoate on intrinsic viscosity

189 Sodium benzoate is a kind of chain transfer agent which could effectively prevent the polymer  
 190 from being cross-linked and ensure growth of the chain length. The effects of the sodium benzoate  
 191 on the intrinsic viscosity of P(AM-DMDAAC) were explored with all other conditions given. As  
 192 shown in Figure 5, the intrinsic viscosity of the polymer exhibited an optimal when the proportion of  
 193 the sodium benzoate was 0.3 ‰ (w/v) and reached the maximum of 3.54 dL/g. When the proportion  
 194 of sodium benzoate was low and it was insufficient to consume excess free radicals or to prevent the  
 195 reaction system from being cross-linked, so the intrinsic viscosity of the polymer was lowered.  
 196 Conversely, when the proportion of sodium benzoate was high, which could lead parts of the free  
 197 radicals in the reaction system was completely consumed, thus hindering the chain growth in the  
 198 polymerization reaction and lowering the intrinsic viscosity of the polymer.

199



200

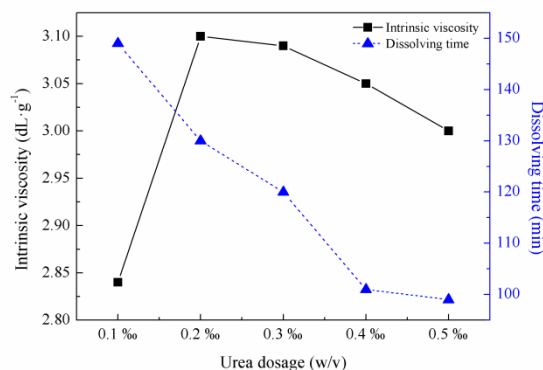
**Figure 5.** Effect of sodium benzoate on intrinsic viscosity

### 201 3.1.6. Effect of urea dose on intrinsic viscosity

202 As shown in Figure 6, the effects of the consumption of the urea on the intrinsic viscosity and  
 203 solubility of P(AM-DMDAAC) showed optimal conditions with increasing urea. When the addition



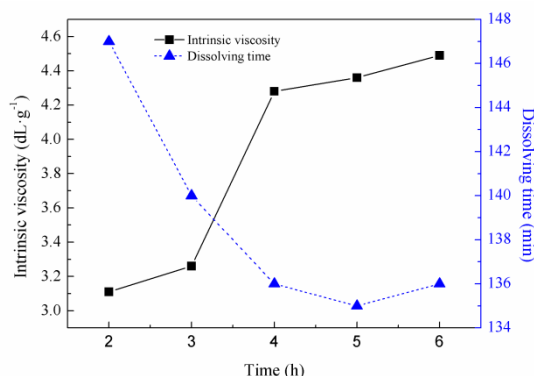
204 of urea was 2 ‰ (w/v), the intrinsic viscosity of the polymer reaches the maximum of 3.1 dL/g, as the  
 205 lower dose of urea assists the reducing agent, which is involved the redox reaction and favors chain  
 206 growth. Thus, the intrinsic viscosity of the polymer increases. When the urea dose is high, chain  
 207 transfer occur, hindering the chain growth and reducing the intrinsic viscosity of the polymer. When  
 208 the using of urea increased from 1 ‰ to 2 ‰, the dissolving time reduces from 149 min to 99 min.



209 **Figure 6.** Effect of urea dose on intrinsic viscosity

### 210 3.1.7. Effect of bath time on intrinsic viscosity

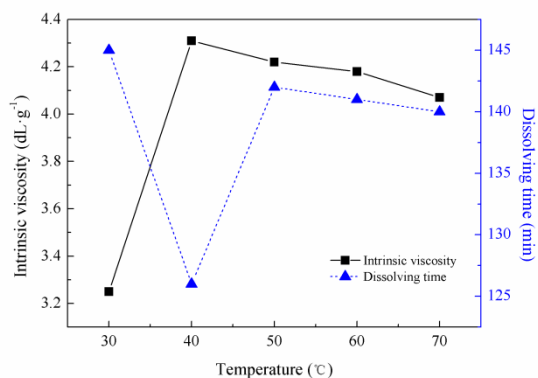
211 The intrinsic viscosity of the polymer increased with water bath time, but the growth reached a  
 212 plateau after extending it as showed in Figure 7. The reason was that when the water bath time is  
 213 short, the polymerization reaction was incomplete and chain propagation was restrained. Thus, the  
 214 intrinsic viscosity of the polymer was low. As the time in the water bath increases after 4 h, the  
 215 intrinsic viscosity of the polymer increased slightly but whilst the degree of chemical reaction was  
 216 high the continual extension of the reaction time not have any great effect on the intrinsic viscosity of  
 217 the polymer. Therefore, the optimal water bath time was identified as 4 h.



218 **Figure 7.** Effect of bath time on intrinsic viscosity

### 219 3.1.8. Effect of reaction temperature on intrinsic viscosity

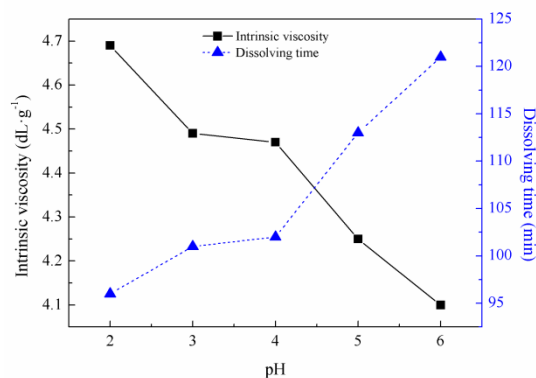
220 The intrinsic viscosity of the polymer exhibited reached a plateau with the increasing reaction  
 221 system temperature as shown in Figure 8. When the water bath temperature was 40 °C, the intrinsic  
 222 viscosity of polymer reached the maximum of 4.3 dL/g, that because both the initiator and the  
 223 activity of the monomer increased with the increased of reaction system temperature. The activity  
 224 and the number of monomer free radicals in the reaction system increased accordingly, which was  
 225 conducive to the polymerization reaction. When the temperature was too high, the polymerization  
 226 reaction became increasingly intense, causing the free radicals of the monomer to cross-link and  
 227 poison the polymerization reaction. Therefore, the optimal water bath temperature was 40 °C.



228 **Figure 8.** Effect of reaction temperature on intrinsic viscosity

### 229 3.1.9. Effect of pH value on intrinsic viscosity

230 As shown in Figure 9, the intrinsic viscosity of the polymer decreased with an increase in pH  
 231 value. When the pH value was 2.0, the intrinsic viscosity of the polymer reached the maximum of 4.7  
 232 dL/g, that because the pH value significantly affected the initiator ammonium persulfate to  
 233 counteract the speed in the polymerization reaction process. When the pH value increased, the  
 234 half-life period of ammonium persulfate becomes shorter with higher initiation rate and  
 235 temperature. The reaction heat accumulated in the reaction system, molecular chains break, and the  
 236 intrinsic viscosity decreased. Therefore, the optimal pH value was 2.



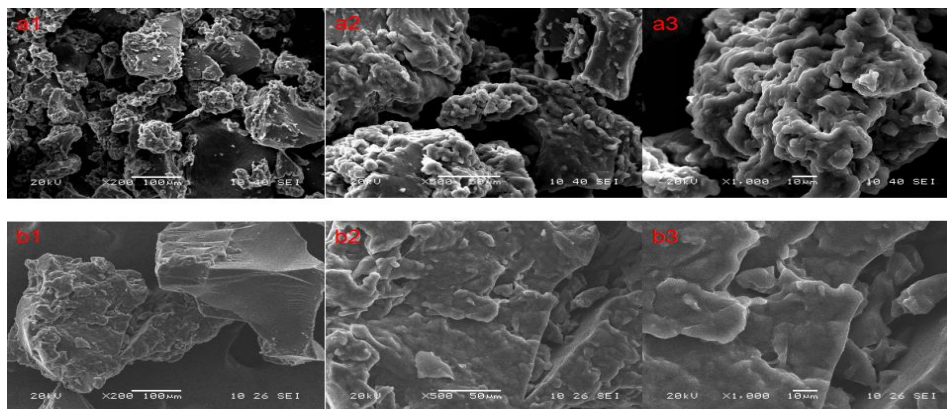
237 **Figure 9.** Effect of pH value on intrinsic viscosity

## 238 3.2. Characterization

### 239 3.2.1. SEM of P(AM–DMDAAC)

240 The Figure 10 illustrates the SEM images of P(AM–DMDAAC) and commercial PAM, thus two  
 241 different surface morphology were observed. It could be seen that the structure of P(AM–  
 242 DMDAAC) was very rough with a large mushroom-shaped cross-cutting structure rather than  
 243 commercial PAM, and possessed bigger specific surface area, which has a strong adsorption and  
 244 bridging capabilities.





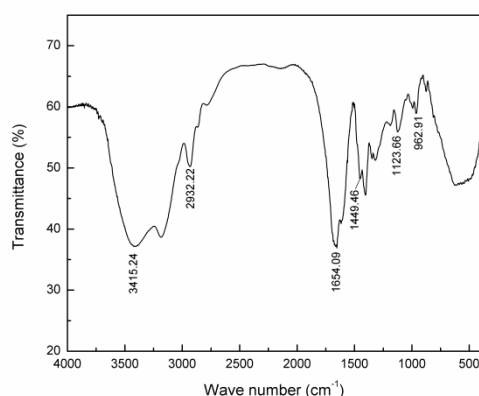
245

246

**Figure 10.** (a) SEM pictures of P(AM-DMDAAC); (b) SEM pictures of PAM

### 247 3.2.2. Infrared spectrum of P(AM-DMDAAC)

248 In Figure 11, the absorption peak at 3415.24  $\text{cm}^{-1}$  is the of  $-\text{NH}_2$  stretching/vibration in the AM  
 249 monomer, at 2932.22  $\text{cm}^{-1}$  is the asymmetric absorption peak of  $-\text{CH}_3$  in the DMDAAC monomer, at  
 250 1654.09  $\text{cm}^{-1}$  is the characteristic absorption peak of  $\text{C}=\text{O}$  in  $-\text{CONH}_2$ , at 1449.46  $\text{cm}^{-1}$  is the  
 251 stretching vibration absorption peak of  $(-\text{CH}_2-\text{N}+(\text{CH}_3)_3$ , and at 962.91  $\text{cm}^{-1}$  is the absorption peak  
 252 of  $\text{N}+\text{R}_4$ , confirming the synthetic polymer is a copolymer of AM and DMDAAC.



253

**Figure 11.** Infrared spectrum of P(AM-DMDAAC)

### 254 3.2.3. $^1\text{H}$ -NMR and $^{13}\text{C}$ -NMR spectra of P(AM-DMDAAC)

255 As shown in Figure 12, the characteristic peak resonance of  $-\text{CH}_2-$  appears with the chemical  
 256 shift at 3.572 ppm in acrylamide; the double-humped characteristic resonance of  $-\text{CH}_3-$  appears  
 257 with the chemical shift at 3.394 ppm; and the peak resonance of  $-\text{NH}_2$  appears with the chemical  
 258 shift above 5 ppm. In the cationic units of the main chain, the characteristic peak of  $-\text{CH}_2-$   
 259 successively appears with the chemical shift at 1.276 ppm and 1.396 ppm, and the characteristic peak  
 260 of  $-\text{CH}-$  successively appears with the chemical shift at 1.818 ppm and 1.976 ppm. In Figure 13, the  
 261 peak with the chemical shift at 179.42 ppm belongs to a characteristic peak resonance of  $\text{C}=\text{O}$  in  $-\text{CONH}_2$  and that of 41.6 ppm belongs to the characteristic peak resonance of  $-\text{CH}_2-$  ( $-\text{CH}-$ ).  
 262



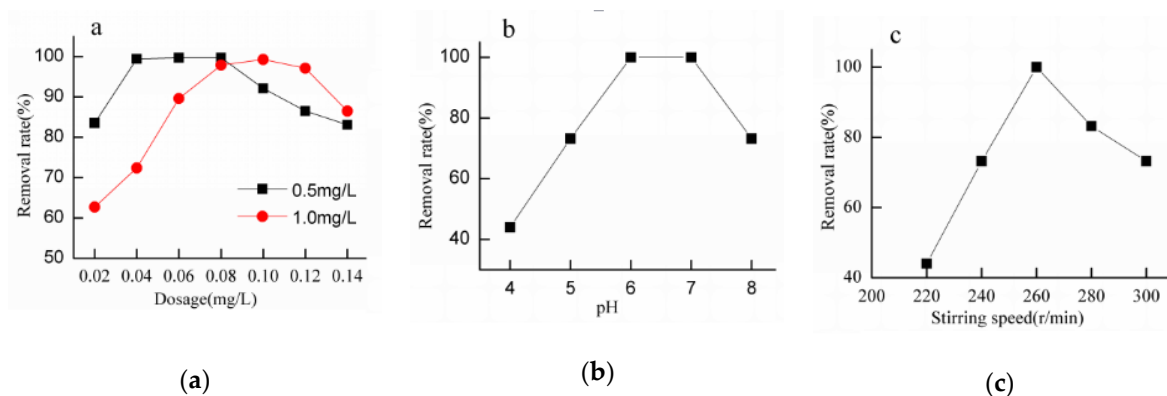
284

**Figure 14.** DSC-TGA of P(AM–DMDAAC)

285 3.3. Validation of the Effectiveness of P(AM–DMDAAC) to remove phenol

286 In this experiment, the effect of P(AM–DMDAAC) dose on the efficiency of phenol removal was  
 287 investigated with the initial phenol concentrations of 0.5 mg/L and 1.0 mg/L. The dose of P(AM–  
 288 DMDAAC) range from 0.02 mg/L to 0.10 mg/L, without adjusting the pH value. The effect of pH  
 289 value on phenol removal efficiency was investigated with the initial phenol concentration of 0.50  
 290 mg/L and the pH value range between 4.0 and 8.0, with the effect of stirring speed on phenol  
 291 removal efficiency investigated with the initial phenol concentration was 0.50 mg/L and the stirring  
 292 speed range from 220 r/min to 300 r/min.

293



294

295 **Figure 15.** a. Effect of dose on removal rate , b. Effect of pH on removal rate, c. Effect of fast stirring  
 296 speed on removal rate

297 Figure 15a shows that the removal efficiency of phenol by P(AM–DMDAAC) was good . The  
 298 phenol removal rate changed from a reasonable value of 83.5 % at 0.02 mg/L P(AM–DMDAAC) to its  
 299 maximum of 99.7% at 0.06 mg/L and subsequently removal efficiency reduces as the P(AM–  
 300 DMDAAC) dose increased with the starting concentration was 0.5 mg/L w/v phenol. At the higher  
 301 starting concentration (1.0 mg/L) removal rate changed from 62.7 % at 0.02 mg/L P(AM–DMDAAC)  
 302 to its maximum of 99.3% at 0.10 mg/L before reducing as before. The explanation of this was that  
 303 when P(AM–DMDAAC) was in excess, the positive charge on the flocs increased, and repulsion  
 304 interaction among flocs was enhanced and so flocs were restabilized and dispersed in treated  
 305 samples. This is because the mechanism of phenol removal in water using P(AM–DMDAAC) is  
 306 mainly by charge neutralization. When increasing the P(AM–DMDAAC) the positive charge density  
 307 in the water body increases and the probability for P(AM–DMDAAC) and phenol contact with each  
 308 other increases. When the optimum dose is exceeded, the positive charges carried by flocculant  
 309 repelled each other, consequently affecting the removal rate.

310 The removal of phenol from the water body using P(AM–DMDAAC) showed an optimum with  
 311 pH (Figure 15b) with the removal efficiency of phenol increasing from a low value of 44.0 % at pH

312 4.0 to its maximum of 99.8 % at pH 7.0 and then decreasing to 73.2 % at pH 8.0. This is due to  
313 neutralization of positive charges carried by the P(AM-DMDAAC) by OH<sup>-</sup>.

314 The effect of stirring speed (Figure15c) provided an optimal condition with removal efficiency  
315 of phenol changing from 44.0 % at 220 r/min to its maximum of 99.8 % at 280 r/min and subsequently  
316 decreasing to 73.2 % at 300 r/min. This may be explained by the sudden increase in the stirring speed  
317 increasing the probability of collision between the P(AM-DMDAAC) and phenol molecules  
318 producing better flocculation. As speed increased, the formed floc structure is destroyed by  
319 turbulence and collision.

#### 320 4. Conclusions

321 A polymeric P(AM-DMDAAC) has been synthesised by acrylamide and dimethyl diallyl  
322 ammonium chloride through microwave assisted radiation. Several parameters affecting the  
323 performance were investigated. FTIR, <sup>1</sup>H NMR and <sup>13</sup>C NMR revealed the structural characteristics  
324 of the P(AM-DMDAAC) which indicated that the synthesis of polymer by MV assisted radiation  
325 was Effective. SEM images provided the apparent morphology of the polymer, which indicated it  
326 had a good adsorption and bridging ability rather than commercial PAM. DTA and TGA results  
327 showed P(AM-DMDAAC) in normal temperature condition is extremely stable. And it was found  
328 that the reaction rate is faster, and the solubility of the P(AM-DMDAAC) is better. In the removal of  
329 phenol experiments, the results exhibited well performance.

330 **Acknowledgments:** The authors are grateful for the financial by the National Natural Science Foundation of  
331 China(Project No. 41502331) and the National Natural Science Foundation of Hunan Province(Project No.  
332 2018JJ3174)

333 **Author Contributions:** Peng Zhang conceived and designed the experiments; Peng Zhang, Dongqin Zhao, Xue  
334 Zhang performed the experiments; Peng Zhang and Dongqin Zhao analyzed the data; Peng Zhang contributed  
335 reagents/materials/analysis tools; Peng Zhang wrote the paper.

336 **Conflicts of Interest:** The authors declare no conflict of interest.

#### 337 References

- 338 1. Bahdod, A., El, A. S., Saoiabi, A., Coradin, T., Laghzizil, A. Adsorption of phenol from an aqueous  
339 solution by selected apatite adsorbents: kinetic process and impact of the surface properties. *Water*  
340 *Res.*, **2009**, *43*, 313-318.
- 341 2. Juang, R. S., Tsai, S. Y. Enhanced biodegradation of mixed phenol and sodium salicylate by *Pseudomonas*  
342 *putida* in membrane contactors. *Water Res.*, **2006**, *40*, 3517-3526.
- 343 3. Liu J. L., Lu W., Zhang F. J., Su X. S., Zhu Y. J., Li R. S., Lu C. Kinetics study of activated persulfate  
344 oxidation of phenol in ground water. *China Envir. Sci.*, **2015**, *35*, 2677-2681.
- 345 4. Abdelwahab, O., Amin, N. K., Elashouky, E. S. Electrochemical removal of phenol from oil refinery  
346 wastewater. *J. Hazard. Mater.*, **2009**, *163*, 711-716.
- 347 5. El-Naas, M. H., Al-Zuhair, S., Alhajja, M. A. Removal of phenol from petroleum refinery wastewater  
348 through adsorption on date-pit activated carbon. *Chem. Eng. J.*, **2010**, *162*, 997-1005.
- 349 6. Kaji, M., Nakahara, K., Ogami, K., Endo, T. Synthesis of a novel epoxy resin containing pyrene moiety  
350 and thermal properties of its cured polymer with phenol novolac. *J. Appl. Polym. Sci.*, **2015**, *75*, 528-535.
- 351 7. Moussavi, G., Mahmoudi, M., Barikbin, B. Biological removal of phenol from strong wastewaters using a  
352 novel msbr. *Water Res.*, **2009**, *43*, 1295-1302.

- 353 8. Busca, G., Berardinelli, S., Resini, C., Arrighi, L. Technologies for the removal of phenol from fluid  
354 streams: a short review of recent developments. *J. Hazard. Mater.*, **2008**, 160, 265-288.
- 355 9. Iurascu, B., Siminiceanu, I., Vione, D., Vicente, M. A., Gil, A. Phenol degradation in water through a  
356 heterogeneous photo-fenton process catalyzed by Fe-treated laponite. *Water Res.*, **2009**, 43, 1313-1322.
- 357 10. Zazo, J. A., Casas, J. A., Mohedano, A. F., Rodriguez, J. J. Semicontinuous fenton oxidation of phenol in  
358 aqueous solution. a kinetic study. *Water Res.*, **2009**, 43, 4063-4069.
- 359 11. Ispas, C. R., Ravalli, M. T., Steere, A., Andreescu, S. Multifunctional biomagnetic capsules for easy  
360 removal of phenol and bisphenol a. *Water Res.*, **2010**, 44, 1961-1969.
- 361 12. Grabowska, E., Reszcyńska, J., Zaleska, A. Mechanism of phenol photodegradation in the presence of  
362 pure and modified-tio<sub>2</sub>: a review. *Water Res.*, **2012**, 46, 5453-5471.
- 363 13. Almeida, F. T., Ferreira, B. C., Moreira, A. L., Freitas, R. P., Gil, L. F., Gurgel, L. V. Application of a new  
364 bifunctionalized chitosan derivative with zwitterionic characteristics for the adsorption of Cu(2+), Co(2+),  
365 Ni(2+), and oxyanions of Cr(6+) from aqueous solutions: kinetic and equilibrium aspects. *J Colloid Interf.*  
366 *Sci.*, **2015**, 466, 297-306.
- 367 14. Zewail, T. M., Yousef, N. S. Chromium ions (Cr 6+, & Cr 3+ ) removal from synthetic wastewater by  
368 electrocoagulation using vertical expanded Fe anode. *J. Electroanal. Chem.*, **2014**, 735, 123-128.
- 369 15. Ye, S., Zhang, M., Yang, H., Wang, H., Xiao, S., Liu, Y., Wang J. H. Biosorption of Cu<sup>2+</sup>, Pb<sup>2+</sup>, and Cr<sup>6+</sup>,  
370 by a novel exopolysaccharide from *Arthrobacter*, ps-5. *Carbohydr. Polym.*, **2014**, 101, 50-56 .
- 371 16. Kadooka H, Jami M S, Tanaka T, Iwata M, J. Mechanism of clarification of colloidal suspension using  
372 composite dry powdered flocculant. *J. Water Pro. Eng.*, **2016**, 11, 32-38.
- 373 17. Zhu, H., Zhang, Y., Yang, X., Liu, H., Shao, L., Zhang, X., Yao J. One-step green synthesis of  
374 non-hazardous dicarboxyl cellulose flocculant and its flocculation activity evaluation. *J. Hazard.*  
375 *Mater.*, **2015**, 296, 1-8 .
- 376 18. Su, Y., Du, H., Huo, Y., Xu, Y., Wang, J., & Wang, L., et al. Characterization of cationic starch flocculants  
377 synthesized by dry process with ball milling activating method. *Int. J. Biol. Macromol.*, **2016**, 87, 34-40.
- 378 19. Fosso-Kankeu, E., Mittal, H., Waanders, F., Ntwampe, I. O., Ray, S. S. Preparation and characterization of  
379 gum karaya hydrogel nanocomposite flocculant for metal ions removal from mine effluents. *Int. J.*  
380 *Environ. Sci. Te.*, **2016**, 13, 711-724.
- 381 20. Wang, T., Yang, W. L., Hong, Y., Hou, Y. L. Magnetic nanoparticles grafted with amino-riched dendrimer  
382 as magnetic flocculant for efficient harvesting of oleaginous microalgae. *Chem. Eng. J.*, **2016**, 297, 304-314.
- 383 21. Weng, B., Xu, F., Garza, G., Alcoutlabi, M., Salinas, A., Lozano, K. The production of carbon nanotube  
384 reinforced poly(vinyl) butyral nanofibers by the forcespinning method. *Polym. Eng. Sci.*, **2015**, 55, 81-87.
- 385 22. Craciun G., Ighigeanu D., Manaila E., Stelescu M. D. Synthesis and Characterization of  
386 Poly(Acrylamide-Co-Acrylic Acid) Flocculant Obtained by Electron Beam Irradiation. *Int. J. Pharm.*, **2015**,  
387 365, 89-99.
- 388 23. Zheng, H., Sun, Y., Zhu, C., Guo, J., Zhao, C., & Liao, Y., Guan Q. Q. Uv-initiated polymerization of  
389 hydrophobically associating cationic flocculants: synthesis, characterization, and dewatering  
390 properties. *Chem. Eng. J.*, **2013**, 234, 318-326.
- 391 24. Zheng, H. L., Sun, Y. J., Guo, J. S., Li, F., Fan, W., Liao, Y., Guan Q. Q. Characterization and evaluation of  
392 dewatering properties of padb, a highly efficient cationic flocculant. *Ind. Eng. Chem. Res.*, **2014**, 53,  
393 2572-2582 .
- 394 25. Zhang P., Ren B. Z., Zhou Y., Liu K. J. Removal of humic acid from aqueous solution by dimethyl diallyl  
395 ammonium chloride and acrylamide. *Asian J. Chem.*, **2013**, 25, 4431-4433 .

- 396 26. Zheng, H. L., Ma, J. Y., Zhu, C. J., Zhang, Z., Liu, L. W., Sun, Y. J., Tang X. M. Synthesis of anion  
397 polyacrylamide under uv initiation and its application in removing dioctyl phthalate from water through  
398 flocculation process. *Sep. & Purif. Technol.*, **2014**, 123, 35-44.